Research Article

Femtosecond laser micromachining optical waveguides on transparent silica xerogels

S.N.C. Santos [a], K.T. Paula [a], F.A. Couto [a], M.H.M. Facure [b,c], D.S. Correa [b,c], C.R. Mendonca [a,*]

[a] University of São Paulo, São Carlos Institute of Physics, 13560-970, São Carlos, SP, Brazil
[b] Nanotechnology National Laboratory for Agriculture (LNNA), Embrapa Instrumentação, 13560-970, São Carlos, SP, Brazil
[c] PPGQ, Department of Chemistry, Center for Exact Sciences and Technology, Federal University of São Carlos, 13565-905, São Carlos, SP, Brazil

ABSTRACT

Femtosecond laser micromachining stands out as an efficient and flexible tool for fabricating optical waveguides, which are key elements in photonics for their ability to confine and direct light propagation. Different materials, from optical glasses to polymers, as well as geometries, have been studied for the fabrication of three-dimensionally inscribed waveguides. This work demonstrates, for the first time, the fabrication of Type II (double-line) waveguides by fs-laser micromachining in a transparent silica xerogel bulk synthesized by the sol-gel process. Specifically, double-line waveguides were fabricated by the multiscan approach at approximately 200 μm below the surface, with a distance between tracks of 20 μm. It was observed fundamental, first and second-order modes of the waveguides at 632.8 nm, which were corroborated by finite elements simulation. Finally, guiding losses of about 2.9 dB/cm were observed for the fundamental mode at 632.8 nm, which is similar to results obtained for Type II waveguides for other materials. Therefore, the intrinsic features of silica xerogel (e. g. low thermal conductivity, non-toxicity, lightness, and high optical transparency) combined to its light guiding ability indicate the potential of micromachined bulk silica xerogels for photonics devices applications.

1. Introduction

Silica xerogels are materials synthesized via the sol-gel process using organic or inorganic materials as precursors and subjected to the slow drying evaporative method at ambient pressure [1]. Silica xerogel can be obtained as bulk material and presents low thermal conductivity, non-toxicity, lightness, and high optical transparency in the UV–Vis and near-infrared region [2,3]. These features allow silica xerogel to be applied in drug delivery systems [4,5], sensors [6], and waveguides [7, 8]. At the same time, femtosecond laser microfabrication has been established as a versatile and efficient technique for fabricating three-dimensional microstructures in transparent materials, such as glasses [9–11], crystals [12,13], polymers [14–16], etc. In this approach, the nonlinear optical interaction limits the light's energy transfer to the material focal volume [17]. A valuable result of such a process is the permanent modification of the refractive index in specific regions, providing a method of fabricating waveguides in the volume of materials [18]. According to the induced change in the refractive index, waveguides fabricated by fs-laser micromachining can be divided into three types, namely Type I, II, and III. Type I waveguides display a subtle

increase in the refractive index at the region irradiated by the laser beam. Type II waveguides, also known as double line waveguides, are obtained by fabricating two tracks parallel to each other. In this case, light confinement is achieved between the tracks where the refractive index is increased, whereas in the tracks it is reduced. Type III waveguides rely on the same refractive index changes as Type II waveguides, but are comprised of several nearby tracks that define the cladding, such that light confinement is obtained in the center where the refractive index is increased [19]. Such waveguides are fundamental components of devices for photonics, finding applications in telecom systems [20], sensors [21], integrated photonics [22], optical isolators [8], and quantum information [23].

In the present work, we demonstrate, for the first time, the fs-laser fabrication of Type II waveguides in silica xerogel bulk samples. The waveguides were fabricated by fs-laser micromachining using the multiscan approach (1, 2, and 4 overlapping passes). Fabrication conditions, specifically pulse energy and beam scanning speed, were studied to determine the optimal parameters. UV–Vis and infrared spectroscopies, as well as thermogravimetric analyzes and differential scanning calorimetry were carried out to characterize the samples. Upon coupling the
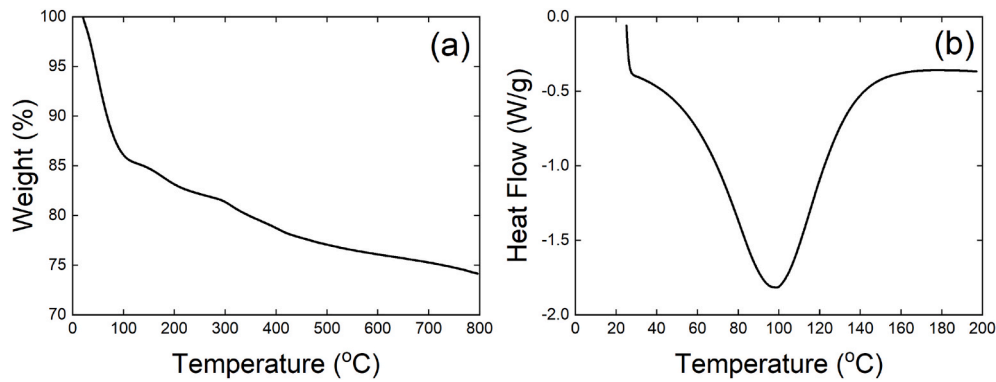
Fig. 1. TG (a) and DSC (a) curves for silica xerogel.

fabricated waveguides with light at 632.8 nm, transversal profiles corresponding to distinct orders were observed.

2. Experimental

Silica xerogels were synthesized by mixing tetraethylorthosilicate (TEOS) (Sigma Aldrich 98%), absolute ethanol (EtOH), deionized water, and hydrochloric acid (HCl) as a catalyst. Initially, a solution containing TEOS, EtOH, and deionized water was prepared and stirred for 10 min at room temperature. Following such procedure, while stirring, 0.1 mol/L of HCl was gradually added to the solution with the molar ratio of TEOS: H_2O:HCl:EtOH of 1:4:0.1:1, The hydrolysis was achieved when the solution was subjected to constant power ultrasonic radiation for 10 min and then stirred for 30 min for complete homogenization. The final solution was placed in molds, covered with a parafilm, kept at 40 °C, and left for gelation for approximately five days. For aging, the gels were maintained under the same conditions for approximately two months. Afterward, the monoliths were subjected to a polishing process. The final sample thickness used for micromachining experiments was 2.5 μm.

The thermal events of the silica xerogel sample were characterized by thermogravimetric analyzes (TGA - Q500 from TA instruments) and differential scanning calorimetry (DSC - Q200 from TA Instruments). For TGA, 5.356 mg of the sample was heated using a platinum pan. The temperature was raised from room temperature to 800 °C using a heating rate of 10 °C/min under nitrogen atmosphere (60 mL/min). DSC measurements were performed from room temperature to 200 °C at a heating rate of 10 °C/min, using an aluminum crucible (6.2 mg sample) and nitrogen atmosphere (50.0 mL/min).

Fourier transform Infrared spectroscopy (FTIR) spectrum of the TEOS xerogel was carried out using a Perkin-Elmer Spectrum 100 FT-IR spectrometer with attenuated total reflectance (ATR) device of diamond-coated zinc selenide crystal. 32 scans in the 4000-500 cm^{-1} spectral range were recorded with a spectral resolution of 4 cm^{-1}. The optical properties of TEOS xerogel were analyzed from 200 nm to 1100 nm using a UV–vis spectrophotometer (Shimadzu, model UV-1800).

Waveguides were micromachined using a femtosecond laser system (diode pumped Yb:KGW) at 1030 nm, operating at 1 kHz and delivering 216-fs pulses, which were focused onto the sample's surface using a 0.65-NA microscope objective while the sample was translated. The sample was positioned in the *x-y-z* plane using three translation stages, allowing moving the sample with constant scan speed in the plane perpendicular to the laser propagation. The micromachining process could be monitored in real-time with a CCD camera and a backlight illumination. All the experiments were carried out in ambient air at atmospheric pressure and room temperature. Type II waveguides were fabricated by using the multiscan approach, in which each track was micromachined by overlapping a different number (1, 2 and 4) of laser passes.
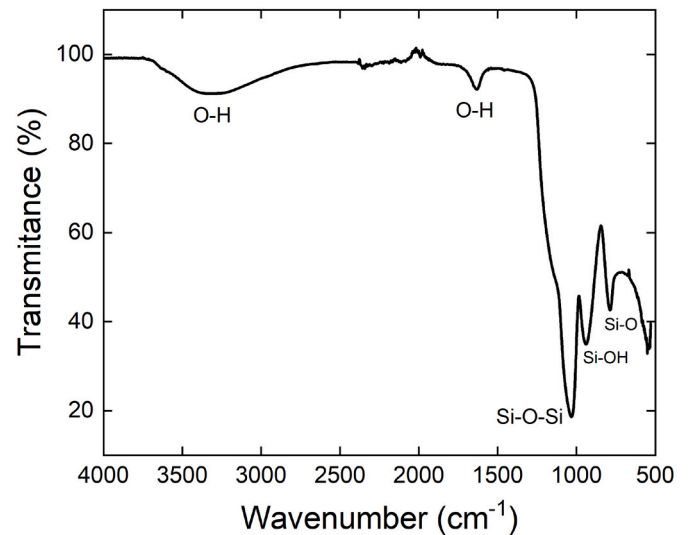

Fig. 2. FTIR spectrum of silica xerogel.

The obtained waveguides were characterized by optical microscopy using a Zeiss LSM 700 microscope. Also, a standard optical coupling system was used to evaluate the guiding properties of the waveguides. This system was composed of a He-Ne laser (632.8 nm), which was coupled in the waveguide by an input objective (NA = 0.65), while an output objective (NA = 0.45) collected the guided light. Transmission losses were determined by measuring the input and output power, taking into account the transmission of all system components. The guided mode profile was imaged with the aid of a CCD.

3. Results and discussion

The TG curve in Fig. 1a shows a mass loss of ca. 15% after heating to approximately 100 °C, which is associated with the endothermic peak that appears in the DSC curve shown in Fig. 1b. This peak corresponds to the elimination of adsorbed water molecules [24]. Furthermore, up to 800 °C, continuous dehydration can be observed without any sign of weight stabilization.

Fig. 2 shows the infrared spectrum of the silica xerogel between 4000 cm^{-1} and 500 cm^{-1}. The IR absorption bands at 3400 cm^{-1} and 1620 cm^{-1} are associated with H-bonded characteristics for vibrations of molecular water [5]. The 1080 cm^{-1} band is attributed to the asymmetric stretching vibration of the Si–O–Si bond, which forms the skeletal SiO_2 network [5,25,26]. The band around 950 cm^{-1} is due to the stretching vibrations of Si–OH [5,25]. At 800 cm^{-1}, the band is attributed to the bond-bending vibration of the Si–O bond in the SiO_2 network [27], and the presence of four-fold siloxane rings appears at
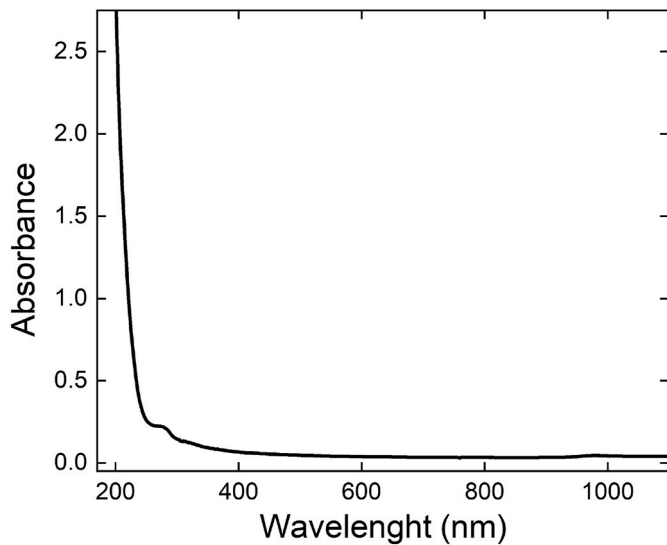
Fig. 3. Absorption spectrum of bulk silica xerogel.

550 cm^{-1} [25].

The optical transparency of the silica xerogels is an essential requirement for developing optical applications. The developed material exhibited high optical transparency up to the UV region with a small absorption band peaking at 280 nm, as indicated in Fig. 3.

A set of experiments was performed to determine the optimal conditions for microfabrication on the silica xerogels and to verify the influence of pulse energy on the process. Groups of lines were micromachined on the silica xerogel surface using a 0.65 NA microscope objective at two different scanning speeds (50 and 100 μm/s, selected from preliminary studies) and different pulse energies, varying from 200 to 500 nJ. Optical microscopy images of the produced lines are shown in
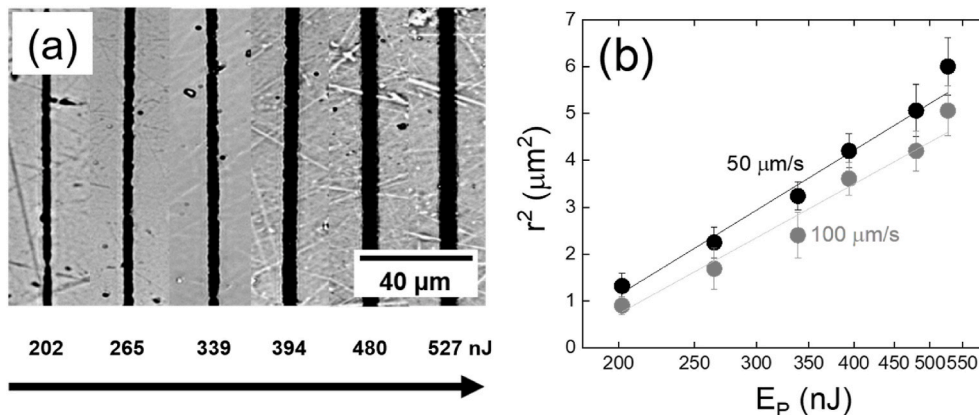
Fig. 4a for the range of pulse energies applied and scanning speed of 100 μm/s, showing better uniformity for higher energies. From a series of images analogous to the ones shown in Fig. 4a, it was possible to obtain an average value of the produced line widths. The half-line width squared (r^2) as a function of pulse energy (E_P) for the two scanning speeds (50 and 100 μm/s) is presented in Fig. 4b. It is possible to observe that as the pulse energy increases, the half-line width of the micromachined line on the silica xerogel surface also increases, exhibiting a linear behavior with the pulse energy in log-scale, following the laser beam Gaussian spatial distribution. Thus, using such scanning speeds and varying the pulse energy, it is possible to fabricate lines with widths (2r) varying from approximately 2 to 5 μm. Following the procedure and expression presented in Ref. [28], by fitting (solid lines) the experimental data in Fig. 4b, we were able to obtain the threshold energies (F_{th}), of (11 ± 1) and (13 ± 1) J/cm^2, respectively, for scanning speeds of 50 μm/s and 100 μm/s.

For producing Type II waveguides, parallel tracks were micromachined using the multiscan method, in which *n* overlapping passes were performed for each track. In this study, in addition to the one-step ($n = 1$) writing, we performed multiscan writing with an overlap of $n = 2$ and 4. Fig. 5 shows optical microscopy images of the top (a) and cross-section (b) top view of the waveguide produced by fs-laser micromachining in silica xerogel for $n = 4$. The waveguides are 7.5-mm long (full sample length) and were produced approximately 200 μm below the sample surface, with tracks separation of 20 μm (determined as the best condition to observe guiding). The pulse energy used for the production of tracks with good homogeneity at the edges along their length was 530 nJ for a scanning speed of 50 μm/s.

Fabricated waveguides were coupled with light at 632.8 nm using the system previously described, and the guided mode profile was imaged with the aid of a CCD camera. Although light guiding was achieved for waveguides fabricated with n = 1, 2, and 4. While for n = 2 only a slightly better light guiding was observed, substantially better confinement was achieved for waveguides produced with n = 4. In

Fig. 4. (a) Optical image showing the line width as a function of the pulse energy used in the laser micromachining process. b) Half-line width squared (r^2) as a function of the pulse energy (E_P) using two different scanning speeds of 50 μm/s (black circles) and 100 μm/s (gray circles).
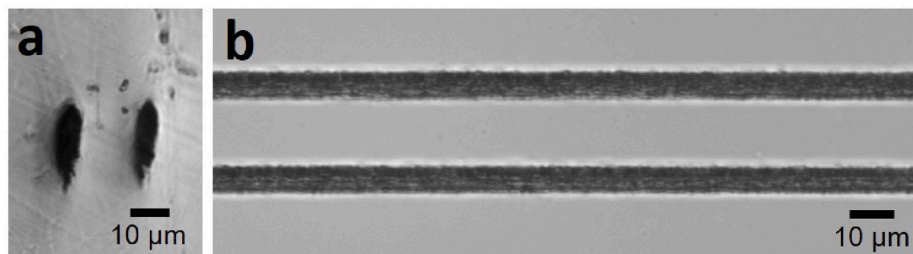

Fig. 5. Optical microscopy images of (a) cross-section view of the input face and (b) top view of waveguides produced in the silica xerogel bulk (n = 4).
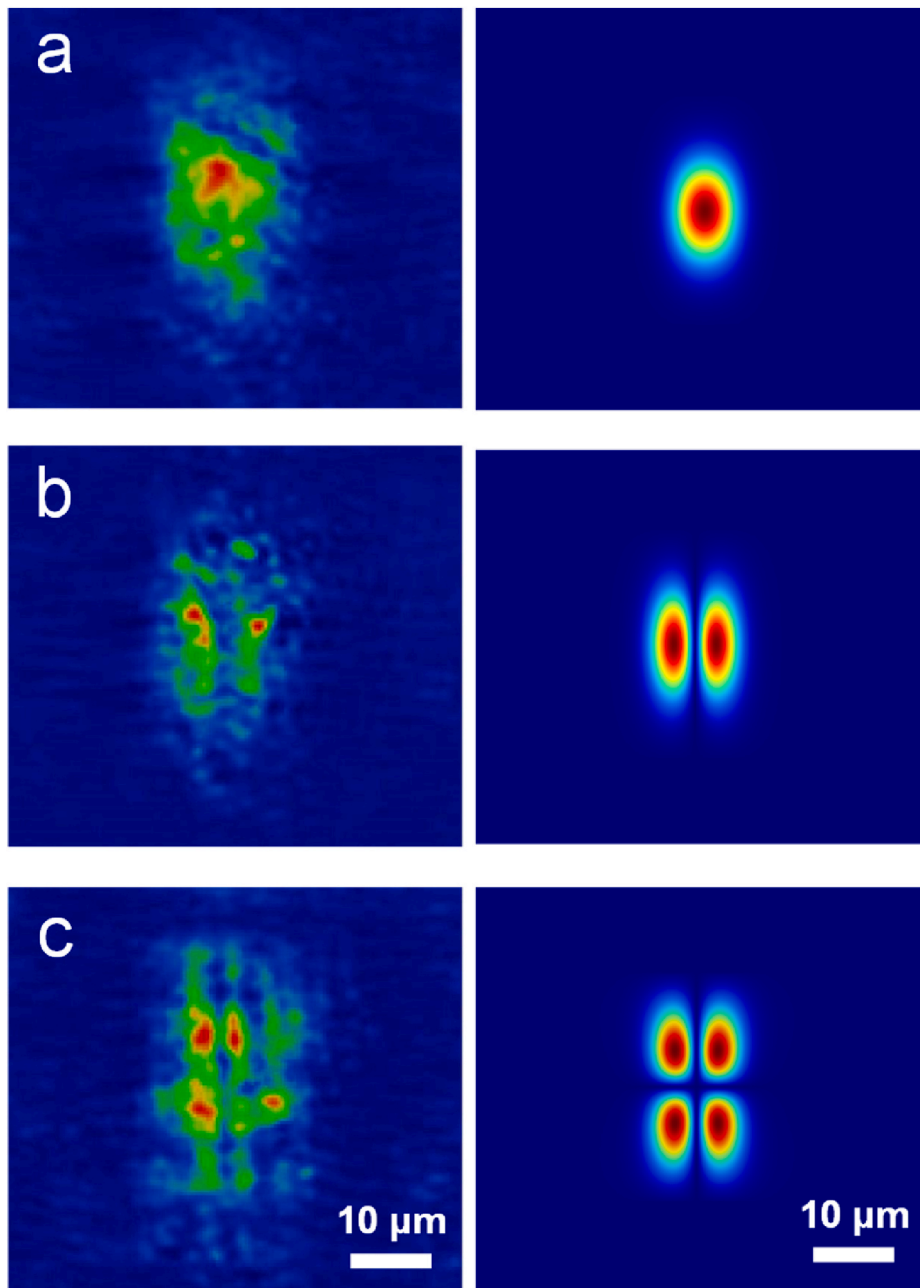
Fig. 6. Experimental (left column) and simulated (right column) near-field of output profile of the light guided at 632.8 nm.

addition, attempts were made to produce waveguides with $n > 4$, which proved to be unfeasible, as the procedure caused extensive cracks and, consequently, the breakage of the sample.

Fig. 6 (left column) displays the experimental mode profiles obtained for three distinct waveguides fabricated with $n = 4$, in which light guiding in different modes were observed. As mentioned before, light confinement in Type II waveguides occurs due to an increase in the refractive index in the region between the micromachined tracks. Finite element calculations, using Comsol Multiphysics, were carried out to perform modal analysis of such waveguide.

For the simulation, the index profile was modeled as a sum of three 2D Gaussians: two symmetrical, negative weighted, accounting for the decrease in the refractive index where the laser focus interacts with the material, and one positive, accounting for the increase of the refractive index at the limits of the laser focus between the two tracks [24]. The mean of all Gaussians was estimated with microscopy images such as

Fig. 5a. Hence, the free parameters were the standard deviation for the x and y dimensions and a weight factor for each distribution.

The simulated mode profiles are shown in Fig. 6 (right column) for guided light at 632.8 nm. Such profiles correspond to fundamental (a), first (b), and second (c) order modes of the waveguide and were obtained by adjusting the simulation parameters until a good correspondence with the experimental results is achieved, indicating an index variation at the order of 10^{-3} at the center of the waveguide. As it can be seen, the modes observed in the fabricated waveguides (Fig. 6 – left column) have a good correspondence to the modeled ones (Fig. 6 – right column), indicating that for such waveguides, depending on the specific features of the structure, such as small imperfections, different guiding modes are achieved.

Guiding losses were estimated by the overlap integral method [29, 30]. Specifically, by measuring the transmission losses and considering the guiding and Fresnel losses at the faces of the sample, the guiding

losses were determined to be (2.9 ± 0.7) dB/cm at 632.8 nm. Such value is in the same order as other ones reported for Type II waveguides. For example, Type II waveguides fabricated in a commercial chalcogenide glass (IG2) displayed propagation losses of ~2.3 dB/cm [31], while those produced in Nd:YAG exhibited propagation losses of 1.6 dB/cm [30]. A better performance was demonstrated for Type II waveguides written in polymethylmethacrylate (PMMA), in which propagation losses of 0.3 dB/cm have been observed [32]. It is noteworthy that combining the interesting features of silica xerogel, such as low thermal conductivity, non-toxicity, lightness, and high optical transparency, with the waveguiding features presented here can be exploited for its used in photonics devices.

4. Conclusions

We demonstrate, for the first time, the use of fs-laser microfabrication to inscribe Type II waveguides in bulk silica xerogels, using a multiscan approach (overlapping passes). Optimal fabrication conditions were determined as being 530 nJ of pulse energy, scanning speed of 50 μm/s, separation between the tracks of 20 μm, and for four-fold overlapping passes, which resulted in better light confinement. Better light confinement was achieved for waveguides fabricated with n = 4, given that the refractive index change increases with the number of passes; for higher n, sample cracking start to occur, making the fabrication unfeasible. The characterization of the waveguide fundamental mode led to a guiding loss (2.9 ± 0.7) dB/cm at 632.8 nm. In addition, the waveguides were able to support fundamental, first- and second-order modes guiding, which were corroborated by the finite elements simulation for a refractive index change of 10^{-3}. Hence, the results presented here successfully demonstrate the fabrication of Type II waveguides in bulk silica xerogels, which can be used for application in optical devices.

CRediT authorship contribution statement

S.N.C. Santos: Conceptualization, Methodology, Validation, Investigation, Writing – original draft, Writing – review & editing. **K.T. Paula:** Conceptualization, Methodology, Validation, Investigation, Writing – original draft, Writing – review & editing. **F.A. Couto:** Formal analysis, Writing – review & editing. **M.H.M. Facure:** Formal analysis, Writing – review & editing. **D.S. Correa:** Formal analysis, Writing – review & editing. **C.R. Mendonça:** Conceptualization, Methodology, Validation, Investigation, Writing – original draft, Resources, Writing – review & editing, Visualization, Supervision, Project administration, Funding acquisition.

Declaration of competing interest

The authors declare that they have no known competing financial interests or personal relationships that could have appeared to influence the work reported in this paper.

Data availability

No data was used for the research described in the article.

Acknowledgments

References

[1] L. Klein, M. Aparicio, A. Jitianu, Handbook of Sol-Gel Science and Technology, second ed., Springer, 2018 https://doi.org/10.1007/978-3-319-32101-1.

[2] M. Marszewski, A. Dashti, P.E. McNeil, M. Fox, V. Wall, D.M. Butts, S.C. King, G. N. Kashanchi, S.H. Tolbert, B. Dunn, L. Pilon, Elastic and plastic mechanical properties of nanoparticle-based silica aerogels and xerogels, Microporous Mesoporous Mater. 330 (2022), 111569, https://doi.org/10.1016/j.micromeso.2021.111569.

[3] Z. Niu, X. He, T. Huang, B. Tang, X. Cheng, Y. Zhang, Z. Shao, A facile preparation of transparent methyltriethoxysilane based silica xerogel monoliths at ambient pressure drying, Microporous Mesoporous Mater. 286 (2019) 98–104, https://doi.org/10.1016/j.micromeso.2019.05.036.

[4] V.J. Hernández-Abad, E.G. Sánchez-González, C. Espinosa-Contreras, R. Marroquín-Segura, J.L.A. Mora-Guevara, Y. Flores-Cabrera, Controlled release of glibenclamide from monolithic silica subdermal implants produced by the sol-gel process and its use for hyperglycaemia treatment in a murine model, Mater. Sci. Eng., C 94 (2019) 1009–1019, https://doi.org/10.1016/j.msec.2018.10.050.

[5] K. Czarnobaj, Preparation and characterization of silica xerogels as carriers for drugs, Drug Deliv. 15 (2008) 485–492, https://doi.org/10.1080/10717540802321495.

[6] D.A. Ilatovskii, V. Milichko, A.V. Vinogradov, V.V. Vinogradov, Holographic sol–gel monoliths: optical properties and application for humidity sensing, R. Soc. Open Sci. 5 (2018), https://doi.org/10.1098/rsos.172465.

[7] S. Nakashima, T. Tanaka, A. Ishida, K. Mukai, Fabrication of optical waveguides inside transparent silica xerogels containing PbS quantum dots using a femtosecond laser, Appl. Phys. Mater. Sci. Process 123 (2017) 1–6, https://doi.org/10.1007/s00339-017-1349-8.

[8] S. Nakashima, R. Okabe, K. Sugioka, A. Ishida, Fabrication of magneto-optical waveguides inside transparent silica xerogels containing ferrimagnetic Fe_3O_4 nanoparticles, Opt Express 26 (2018), 31898, https://doi.org/10.1364/oe.26.031898.

[9] S.N.C. Santos, G.F.B. Almeida, J.M.P. Almeida, A.C. Hernandes, C.R. Mendonça, Waveguides fabrication by femtosecond laser in Tb^{3+}/Yb^{3+} doped CaLiBO glasses, Opt Laser. Technol. 140 (2021), https://doi.org/10.1016/j.optlastec.2021.107030.

[10] X. Long, J. Bai, Laser action from a femtosecond laser written Yb: phosphate glass waveguide, Optik 249 (2022), 168308, https://doi.org/10.1016/j.ijleo.2021.168308.

[11] J.M.P. Almeida, L. De Boni, W. Avansi, C. Ribeiro, E. Longo, A.C. Hernandes, C. R. Mendonça, I. De Física, D.S. Carlos, U.D.S. Paulo, S. Carlos, Generation of Copper Nanoparticles Induced by Fs-Laser Irradiation in Borosilicate Glass, vol. 20, 2012, pp. 15106–15113, https://doi.org/10.1364/OE.20.015106.

[12] Y.F. Bao, T. Liu, W.J. Kong, H.Q. Luo, Y. Liu, F.R. Liu, L. Cheng, Enhanced Raman spectra in femtosecond laser inscribed $Yb:YVO_4$ channel waveguides, Front. Physiol. 9 (2021) 1–5, https://doi.org/10.3389/fphy.2021.758071.

[13] Q. Liu, M. Geng, Y. Yu, Q. Chen, J. Qiu, Z. Zhang, Femtosecond laser direct written waveguides and laser induced-effects in erbium-doped GYSGG crystals, Opt. Mater. Express 10 (2020) 724, https://doi.org/10.1364/ome.385278.

[14] S. Hayashi, K. Tsunemitsu, M. Terakawa, Laser direct writing of graphene quantum dots inside a transparent polymer, Nano Lett. 22 (2022) 775–782, https://doi.org/10.1021/acs.nanolett.1c04295.

[15] G.L. Roth, S. Kefer, S. Hessler, C. Esen, R. Hellmann, Polymer photonic crystal waveguides generated by femtosecond laser, Laser Photon. Rev. 15 (2021) 1–8, https://doi.org/10.1002/lpor.202100215.

[16] C. Mendonca, D. Correa, F. Marlow, T. Voss, P. Tayalia, E. Mazur, Three-dimensional fabrication of optically active microstructures containing an electroluminescent polymer, Appl. Phys. Lett. 95 (2009) 113309, https://doi.org/10.1063/1.3232207.

[17] K.C. Phillips, H.H. Gandhi, E. Mazur, S.K. Sundaram, Ultrafast laser processing of materials: a review, Adv. Opt Photon 7 (2015) 684–712, https://doi.org/10.1364/AOP.7.000684.

[18] F. Chen, J.R. Vázquez de Aldana, Three-dimensional Femtosecond Laser Micromachining of Dielectric Crystals for Photonic Waveguiding Applications, Proc. SPIE, 2015, pp. 1–9, https://doi.org/10.1117/12.2182861.

[19] W. Nie, J.R. Vázquez de Aldana, F. Chen, Dual-line optical waveguides in Cu: KNSBN crystal fabricated by direct femtosecond laser writing, Opt. Eng. 54 (2015), 097106, https://doi.org/10.1117/1.oe.54.9.097106.

[20] M.R. Krogstad, S. Ahn, W. Park, J.T. Gopinath, Optical characterization of chalcogenide Ge-Sb-Se waveguides at telecom wavelengths, IEEE Photon. Technol. Lett. 28 (2016) 2720–2723, https://doi.org/10.1109/LPT.2016.2615189.

[21] M. Vlk, A. Datta, S. Alberti, H.D. Yallew, V. Mittal, G.S. Murugan, J. Jágerská, Extraordinary evanescent field confinement waveguide sensor for mid-infrared trace gas spectroscopy, Light Sci. Appl. 10 (2021), https://doi.org/10.1038/s41377-021-00470-4.

[22] B. Desiatov, A. Shams-Ansari, M. Zhang, C. Wang, M. Lončar, Ultra-low-loss integrated visible photonics using thin-film lithium niobate, Optica 6 (2019) 380, https://doi.org/10.1364/optica.6.000380.

[23] B. Sotillo, V. Bharadwaj, J.P. Hadden, S. Rampini, A. Chiappini, T.T. Fernandez, C. Armellini, A. Serpengüzel, M. Ferrari, P.E. Barclay, R. Ramponi, S.M. Eaton, Visible to infrared diamond photonics enabled by focused femtosecond laser pulses, Micromachines 8 (2017) 1–10, https://doi.org/10.3390/mi8020060.

[24] Y. Maeda, Y. Hayashi, J. Fukushima, H. Takizawa, Sonochemical effect and pore structure tuning of silica xerogel by ultrasonic irradiation of semi-solid hydrogel, Ultrason. Sonochem. 73 (2021) 105476, https://doi.org/10.1016/j.ultsonch.2021.105476.

[25] X. Rios, P. Moriones, J.C. Echeverría, A. Luquín, M. Laguna, J.J. Garrido, Characterisation of hybrid xerogels synthesised in acid media using methyltriethoxysilane (MTEOS) and tetraethoxysilane (TEOS) as precursors, Adsorption 17 (2011) 583–593, https://doi.org/10.1007/s10450-011-9331-9.

[26] U.T. Uthappa, G. Sriram, V. Brahmkhatri, M. Kigga, H.Y. Jung, T. Altalhi, G. M. Neelgund, M.D. Kurkuri, Xerogel modified diatomaceous earth microparticles for controlled drug release studies, New J. Chem. 42 (2018) 11964–11971, https://doi.org/10.1039/c8nj01238e.

[27] S. Ibrahem, H. Ibrahem, Preparation and study properties of xerogel silica using sol-gel method, Int. J. Appl. or Innov. Eng. Manag. 2 (2013) 111–116.

[28] J.M. Liu, Simple technique for measurements of pulsed, Gaussian-beam spot sizes 7 (1982) 196–198, https://doi.org/10.1364/OL.7.000196.

[29] R. Osellame, N. Chiodo, G. Della Valle, S. Taccheo, R. Ramponi, G. Cerullo, A. Killi, U. Morgner, M. Lederer, D. Kopf, Optical waveguide writing with a diode-pumped femtosecond oscillator. https://doi.org/10.1364/OL.29.001900, 2004, 29 (2004) 1900-1902.

[30] T. Calmano, J. Siebenmorgen, O. Hellmig, K. Petermann, G. Huber, Nd:YAG waveguide laser with 1.3 W output power, fabricated by direct femtosecond laser writing, Appl. Phys. B Laser Opt. 100 (2010) 131–135, https://doi.org/10.1007/s00340-010-3929-6.

[31] W. Hu, M. Kilinc, W. Gebremichael, C. Dorrer, J. Qiao, Morphology and waveguiding properties of ultrafast-laser-inscribed type-II waveguides in IG2, Opt. Mater. Express 12 (2022) 360, https://doi.org/10.1364/ome.447213.

[32] W.M. Pätzold, A. Demircan, U. Morgner, Low-loss curved waveguides in polymers written with a femtosecond laser, Opt Express 25 (2017) 263–270, https://doi.org/10.1364/oe.25.000263.